Strategies for Modeling Friction in Gear Dynamics

Manish Vaishya

Rajendra Singh
e-mail: singh.3@osu.edu

Department of Mechanical Engineering,
The Ohio State University,
Columbus, OH 43210-1107

Sliding friction between meshing teeth is one of the primary excitations for noise and vibration in geared systems. Yet, there exist very limited studies on this topic. This paper proposes new modeling strategies for incorporating friction in the dynamic analysis of a gear pair. First, some tribological issues are discussed for estimation of the friction forces under different operating conditions. Second, modeling procedures and results are compared for linear time-invariant, linear time-varying and non-linear time-varying formulations. Criteria such as energy balance, system complexity and desired solution methodology are discussed. Finally, sample results from the various analyses along with their benefits and limitations are examined. [DOI: 10.1115/1.1564063]

Introduction

Most practical gear meshes encompass complex friction characteristics in the tooth contact zone, which are comprised of mixed lubrication conditions [1,2]. Kelley and Lemanski [2] derived the equations for prediction of the coefficient of friction under boundary lubrication, and this formulation is still widely used. Alternative formulations can be found in a summary prepared by Martin [1]. Such empirical knowledge has been incorporated in various forms in gear dynamic studies, but many simplifying representations such as the Coulomb model [3–5] have been employed. For instance, Radzimovsky and Mirarefi [3] proposed a dynamic model in the torsional direction for a four-degree of freedom gear system. Iida et al. [4] studied the shaft vibrational response in the tooth sliding direction. Borner and Houser [5] extended this to helical gears to predict friction force on the whole tooth surface under quasi-static conditions. Recently, some dynamic models have been proposed which use the fluid film calculations to estimate the friction properties [6,7]. The majority of studies that include friction in gear dynamics have adopted numerical methods. A more rigorous analytical treatment was offered [8] by us that explicitly included the periodic nature of friction in conjunction with the time-varying mesh properties.

In the absence of friction mechanism, extensive gear dynamic models exist. Comprehensive and critical reviews of literature have been reported by Ozguven and Houser [9], and Blankenship and Singh [10]. Many additional dynamic phenomena, such as super-harmonic response, unstable regimes, multiple solutions, sub-harmonic resonance and angular modulation emerge, when the time-varying or nonlinear contact characteristics are included. Consequently, alternate methodologies such as Galerkin techniques for clearance nonlinearity [11,12] or numerical simulation methods [6,13] have been used. Geared systems are also characterized by the existence of regimes of dynamic instabilities, caused by the large fluctuations in mesh compliance [14]. Yet, none of the studies explicitly considered sliding resistance in the stability analysis.

Based on the literature review, it is abundantly clear that among the different kinds of non-linearities in the gear system, such as clearance, spatial variations and sliding friction, the effect of friction is the least understood. Certain unique characteristics of gear tooth sliding make it a potentially dominant factor. For instance, due to the reversal in direction during meshing action, friction is associated with a large oscillatory component, which causes a higher bandwidth in the system response. Furthermore, it becomes more significant at high values of torque and lower speeds, due to the tribological characteristics as well as due to higher force transmissibility in the sliding direction. With this motivation, the following objectives have been identified for this article: (1) propose alternative strategies for modeling of sliding friction phenomenon, (2) compare mathematical models for attributes like underlying assumptions, computational and analytical solution needs, energy conservation and degrees of freedom, and (3) investigate the essential differences between linear and nonlinear, as well as time-invariant and time-varying formulations.

Problem Formulation

Sliding friction can affect the gear system dynamics in many distinct ways, such as an excitation, as a periodic system parameter, as a nonlinear coupling agent or as a source of energy dissipation. First, sliding friction can be modeled as an external excitation with the same fundamental period as the gear meshing cycle [3,5]. If sliding mechanism is formulated based on the dynamic mesh force [6,8], then friction terms participate as time-varying parameters in the system. Alternatively, an implicit non-linearity occurs due to the dependence of friction on the instantaneous sliding velocity, and that introduces a dynamic coupling between system parameters and sliding mechanism. Finally, sliding resistance can influence the system with its damping characteristics, as discussed by Iida et al. [4] and Velex and Cahouet [6]. Our paper will discuss some of these methods, using a simplified torsional model of a spur gear pair operating under sliding friction and time-varying mesh parameters. For the purpose of illustration, the auxiliary components of the gearbox are ignored, so that the parametric and non-linear effects in the meshing zone are accentuated. Mesh stiffness is assumed to follow a periodic variation in the form of rectangular pulses. The coefficient of friction (μ) is represented as an idealized mathematical entity. The normal contact load is assumed to be equally distributed amongst all the teeth in contact. For this gear pair, other non-linearities such as tooth backlash and spatial domain dependency of mesh parameters are neglected.

Figure 1 shows a generalized model for a single mesh gear system, where the pinion and gear are represented by their base circles with radii R (subscripts p and g represent the pinion and gear respectively). Mesh stiffness (k) is a result of Hertzian deformation as well as the cantilever bending of the teeth, and c is the associated damping coefficient. Profile deviations on the teeth surfaces, either by design or due to manufacturing errors, constitute a displacement excitation at the mesh, referred to as the unloaded static transmission error $\varepsilon(t)$. Sliding on the gear tooth surface causes a frictional force F_f along the off-line of action direction or η-direction, and a torque T_f about both the gear axes. In our

Contributed by the Power Transmission and Gearing Committee for publication in the JOURNAL OF MECHANICAL DESIGN. Manuscript received March 2001; revised September 2002. Associate Editor: R. F. Handschuh.

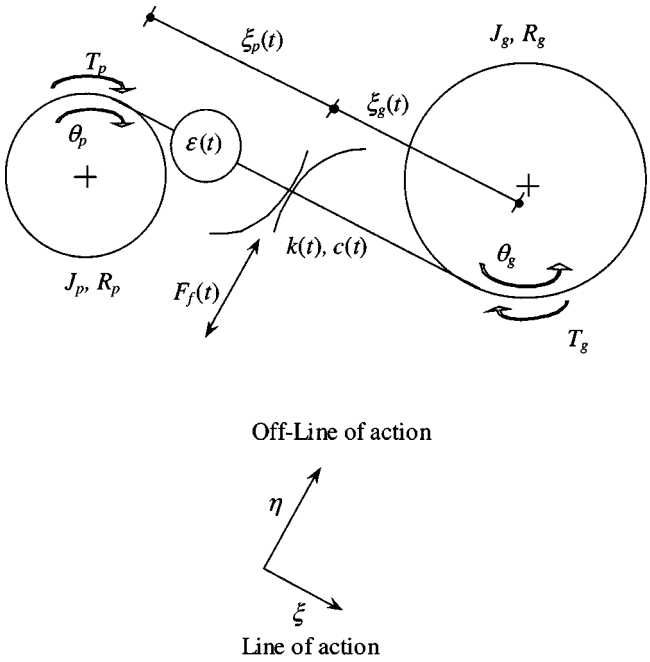

Fig. 1 Torsional model of gear pair with friction force

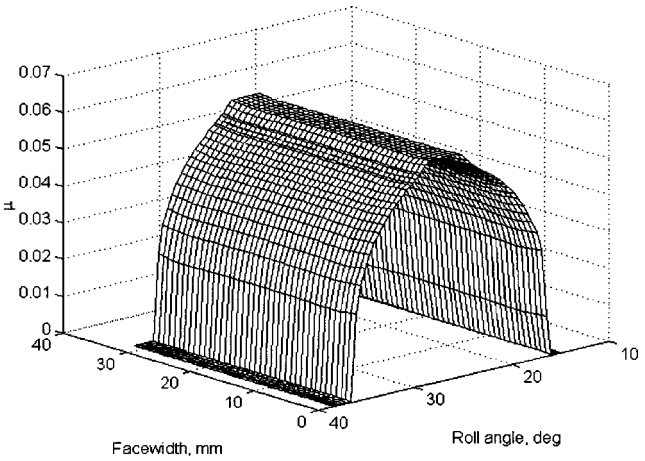

Fig. 2 Typical variation in μ over the entire surface of a spur gear tooth

example [15], a pair of spur gears is considered with linear profile modification; the key gear design parameters are shown in Table 1.

During the gear meshing action, the tooth contact point moves along the line of action (ξ direction), and T_f changes continuously due to linearly varying values of $\xi_p(t)$ and $\xi_g(t)$. External torques T_p and T_g operate upon the pinion and gear respectively. The gears rotate with mean angular speeds Ω, whereas θ represents the angular displacement from the mean position. For any gear tooth pair i in contact, the sliding velocity V_s at the mesh interface is given as follows, where α is the gear roll angle.

$$V_{s,i} = \alpha_{g,i}\xi_g(\Omega_g + \dot{\theta}_g) - \alpha_{p,i}\xi_p(\Omega_p + \dot{\theta}_p) \tag{1}$$

The magnitude and direction of V_S govern the friction at the surface. For most practical designs of spur gears, the profile contact ratio Γ has a value between 1.0 and 2.0, implying that two teeth are in contact for (Γ-1) fraction of total time, and a single tooth is transmitting the torque during the rest of the mesh cycle. In this study, the beginning of the mesh cycle at $\alpha = \alpha_0$ is defined to be coincident with the initiation of contact for the second tooth. As the gears roll, the first tooth leaves contact and there is a significant reduction in $k(t)$. Consequently, the load shared by the 2nd tooth undergoes a corresponding increase. Till this position ($\alpha = \alpha_a$) is reached, both V_s and F_f on the two pairs of teeth act in opposite directions. The second critical point occurs at α_b when the zone of contact passes through the pitch point, and the direction of V_S for tooth 2 reverses. Finally, the third gear tooth comes into engagement at α_c and this constitutes one gear mesh cycle.

Gear Tribology Factors

When the gears operate near their maximum load capacity, very high contact pressure occurs at the mesh interface. This may lead to a partial breakdown of the lubricant film at the surface, thus resulting in two commonly encountered regimes, the elastohydrodynamic (EHD) and boundary lubrication [1]. Furthermore, tribological parameters, such as the radius of curvature ρ and V_S, change over the whole gear tooth surface. Under EHD conditions, μ is a function of the surface velocity, curvature ρ and normal contact load N on the mating surfaces, such that $\mu = f(V_S, N, V_R, T_L, \rho, \eta_0 \ldots)$. Here V_R is the rolling velocity at the surface, η_0 is the lubricant dynamic viscosity and T_L is the fluid inlet temperature. Conversely, mixed lubrication conditions are characterized by partial asperity contact, and surface finish R_q becomes an additional parameter influencing friction properties.

A unified principle that can represent μ under all conditions has eluded most researchers. Many alternative formulations have been proposed, based on different lubrication regimes, as summarized by Martin [1]. Equation (2) shows the expression derived by Kelley and Lemanski [2] for mixed lubrication conditions, where C_1, C_2 and C_3 are empirical coefficients and w is the distributed load per unit length of contact.

$$\mu = C_1 \frac{1}{1 - C_2 R_q} \log_{10}\left[\frac{C_3 w}{\eta_0 V_s V_R^2 (\rho_p + \rho_g)^2}\right] \tag{2}$$

Thus, the expression for μ is a complex non-linear function of load distribution, surface kinematics and tribological factors. Furthermore, due to their empirical nature, such expressions are valid only for a certain range of parameters. A typical variation in μ over the whole tooth surface of a spur gear is shown in Fig. 2, based on Eq. (2). The load distribution is estimated using the finite element method [16]. This plot demonstrates that there is a significant variation in the value of μ as the point of contact moves over the whole tooth surface.

Clearly, such a formulation precludes much of analytical treatment and simpler models must be adopted for μ. It has been shown [6,10] that the dynamic response of the gear system is dominated by the reversal in direction of the friction force, and the actual variation in the magnitude does not play a crucial role. Hence the simplest case incorporates the Coulomb model with $\mu = \mu_0 \,\mathrm{sgn}(V_S)$, where μ_0 is a material property. To maintain continuity at the pitch point where $V_S = 0$, a trigonometric function is often used instead, as shown in Eq. (3). This may also be a more realistic representation of a physical gear mesh. The reference parameter V_0 is applied for nondimensionalization as well as to control the slope of the function near the pitch point.

$$\mu_K = (2\mu_0/\pi)\tan^{-1}(V_S/V_0) \tag{3}$$

In order to observe the influence of friction on the dynamic response of the gear pair, some preliminary experiments were con-

Table 1 Gear design parameters and critical time instant values for one mesh cycle

Number of teeth Π_p, Π_g	25, 31	Input torque T_p	226 Nm
Center distance	88.9 mm	k_{mean} (MN/m)	568
Profile contact ratio Γ	1.433	$k_{\max}$ (MN/m)	720

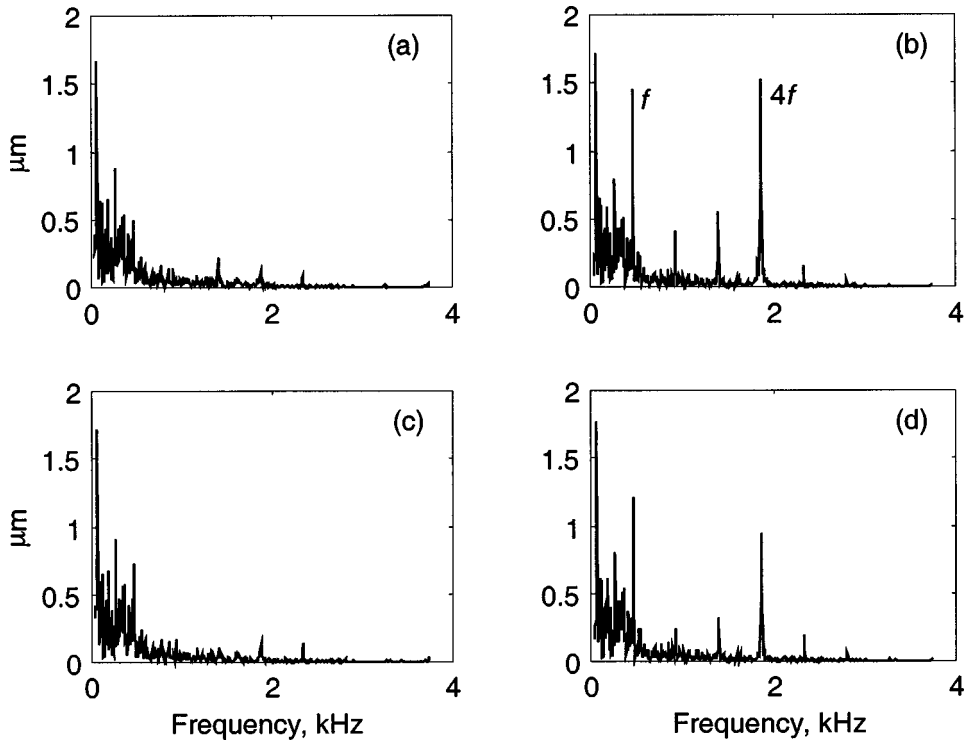

Fig. 3 Measured pinion deflection in traction (ξ) and sliding (η) direction for T_p=102 Nm, Ω_p=1000 rpm. (*a*) Low η_0 lubricant, ξ-direction; (*b*) Low η_0 lubricant, η-direction; (*c*) High η_0 lubricant, ξ-direction; (*d*) High η_0 lubricant, η-direction.

ducted. Figures 3(*a*)–(*b*) show the gear body displacements due to friction forces and those due to $\varepsilon(t)$, which includes the parametric excitation by variations in meshing stiffness. Additionally, a second lubricant is used (see Figs. 3(*c*)–(*d*) with high viscosity, resulting in a low μ value. It is apparent that the dynamic effects in the η-direction can be significant, even dominant under this condition of high torque and low surface speed. Lower viscosity lubricants give a higher friction force, as predicted by Eq. (2), due to the presence of mixed lubrication conditions. Furthermore, sliding forces have a larger presence in higher harmonic zone (f represents the mesh frequency) of the spectrum. These results establish the considerable dynamic effects in the sliding direction, which in part provides the motivation for this research.

Estimation of Friction Force

For any roll position α in the gear mesh, the total friction force or torque can be determined by integration over the whole tooth as well as over all the teeth in contact. The friction force on area dS is first derived from μ and the surface contact pressure P_i. Thus for each gear tooth i in contact:

$$F_{f,i}(t) = \oint_i \mu_i(t,S) P_i(t,S) dS; \quad \text{in the } \eta\text{-direction.} \tag{4}$$

$$T_{f,i}(t) = \oint_i \mu_i(t,S) P_i(t,S) \xi_i(t,S) dS \tag{5}$$

Two assumptions are commonly made when simplifying the expressions in Eqs. (4–5). First, for each tooth, the width of the contact zone in the profile direction is small in comparison to the facewidth, so that the interface can be modeled as a line contact. Secondly, by appropriate design modifications in the gear surface, the variation in contact pressure along the facewidth can be minimized [16]. With these two assumptions, a well designed gear pair with no misalignment will have a fairly uniform coefficient of friction, as seen in Fig. 2. Also for a spur gear, ξ_i is constant across the facewidth due to kinematic constraints and thus Eqs. (4–5) can be written in discrete form as follows:

$$F_f = \sum_{i=1}^{\lceil \Gamma \rceil} F_{f,i} = \sum_{i=1}^{\lceil \Gamma \rceil} \mu_i F_{\text{mesh},i} \tag{6}$$

$$T_f = \sum_{i=1}^{\lceil \Gamma \rceil} T_{f,i} = \sum_{i=1}^{\lceil \Gamma \rceil} \mu_i F_{\text{mesh},i} \xi_i \tag{7}$$

Here $\lceil \Gamma \rceil$ represents the maximum number of teeth that are in contact at any given instant in the mesh cycle. Note that in gear dynamic models that ignore friction, only the sum of line of action forces needs to be included. Conversely, when friction dynamics are considered, the true load distribution among the teeth must be determined for calculation of F_f and μ. For this torsional system, the mesh force F_{mesh} under dynamic conditions is given by:

$$F_{\text{mesh},i} = k_i(t)(\delta(t) - \varepsilon_i(t)) + c_i(t)(\dot{\delta} - \dot{\varepsilon}_i) \tag{8}$$

Here δ is the relative displacement of the gears, known as the dynamic transmission error (DTE) and is given by $\delta = R_p\theta_p - R_g\theta_g$. As a further simplification, the relative load distribution among the teeth can be assumed to be in proportion to the quasi-static load distribution, irrespective of the individual variation of k_i and ε_i. This allows one to express the individual tooth load under dynamic conditions in terms of time-invariant load distribution factors σ_i's, in the form of Eq. (9). The obvious advantage of this approach is that each gear tooth does not need to be modeled separately in the dynamic equations. Thus $F_{\text{mesh},i}/F_{\text{mesh},j}$ = constant, $\forall i \neq j$ and $F_{\text{mesh},i} = \sigma_i F_{\text{mesh}}$, $\forall t$, where $\sigma_i \leqslant 1$. Then the Eq. (7) for friction torque becomes:

$$T_f = F_{\text{mesh}} \sum_{i=1}^{\lceil \Gamma \rceil} \sigma_i \mu_i \xi_i \tag{9}$$

Equations (6–9) show that the friction force consists of terms that include products of μ and δ. Thus, μ participates in the sys-

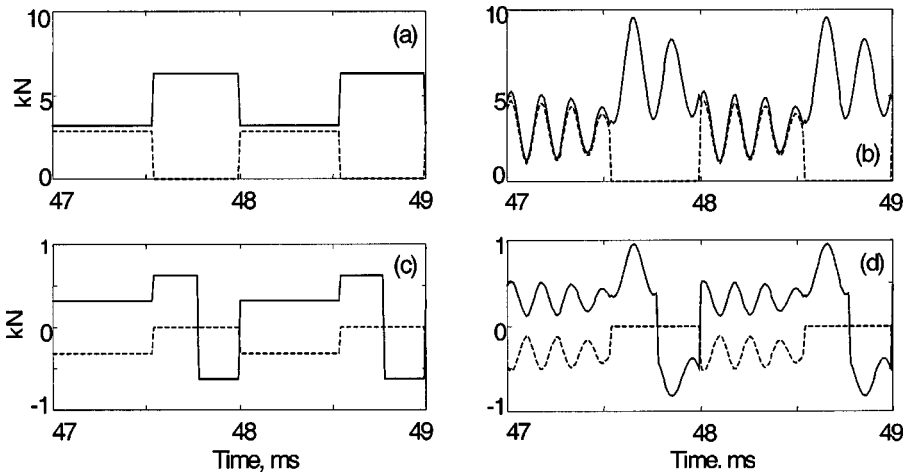

Fig. 4 Simulated mesh and friction forces on the two teeth when static and dynamic mesh forces are considered at $\Gamma=1.532$, $\mu=0.1$, $\zeta=0.01$, $\Omega_p=2400$ rpm (non-resonant condition). (*a*) Mesh load using *N*; (*b*) Mesh load using F_{mesh}; (*c*) F_f using *N*; (*d*) F_f using F_{mesh}. Key: — — — 1st tooth in mesh, —— 2nd tooth in mesh (2 mesh cycles shown).

tem equations as a dynamic parameter. Alternatively, F_{mesh} can be replaced by the quasi-static load distribution N on the tooth surfaces, and then friction becomes purely an external excitation. Furthermore, μ is also assumed unaffected by the dynamic response and is determined from the quasi-static meshing conditions. Figure 4 shows the mesh and friction force on each tooth for these two cases, when a damping ratio $\zeta=0.01$ is used. The frequency spectra of friction force (Figs. 5(*a*)–(*b*) for these two cases only showed a minimal difference. The effect of approximating F_{mesh} by N_i is more apparent near resonant conditions, because of the high dynamic factor. In Figs. 5(*c*)–(*d*), the response of the gear pair is computed near one of the super-harmonic resonances. Under these conditions, spectra of F_f calculated using $F_{\text{mesh}}(x,t)$ shows a large amplitude as compared that with $N(t)$.

Energy Considerations and Degrees of Freedom

A gearbox comprises of numerous elements that include bearings, compound shafts, couplings and external inertias. In order to analyze all the components, a very large and intricate model will be required. Despite such complexities, discrete lumped parameters models may yield sufficient accuracy for most practical applications [9]. The extent of discretization will naturally depend upon the frequency range of interest, modal separation, physical properties of the components, multi-directional coupling of forces and external excitations. For instance, inclusion of translational dynamic effects of friction usually generates two additional displacements in the sliding (η) direction. Secondly, most of the components in a gearbox can be fairly well approximated by linear dynamic elements such as mass, damper or spring, and most significant nonlinearities as well as time-varying properties occur within the gear meshing zone. Hence, a compact yet mathematically tractable system gives a much better insight into these physical phenomena, and the results of this analysis can then be easily extrapolated to higher dimensional systems.

In the simplest form of analysis, the gear pair assumes a purely torsional configuration with 2 degrees of freedom θ_p and θ_g (Fig. 1). Furthermore, due to the fact that such a dynamic system will always be semi-definite, most researchers have reduced this to a single variable δ. Such a substitution is possible because θ_p and θ_g are not mutually independent response variables in the equations of motion. Thus, this procedure is valid for most models that simulate the gear meshing along the line of action (ξ) direction. However, in certain cases, θ_p and θ_g may appear explicitly in the equations of motion and as a consequence, a minimum of two degrees of freedom must be considered. Oh et al. [17] have shown one such example resulting from spatial domain variations in meshing stiffness, where both δ and the mean displacement govern the meshing properties. Another important scenario that necessitates an extra variable occurs when sliding friction is formulated as a non-linear function of the tooth sliding velocity. The first derivatives of θ_p and θ_g appear explicitly in the definition of μ, and two basis solutions are required. This leads to the recurrence of the problem of semi-definiteness, which must now be resolved to attain a steady response.

In order to make the system of Fig. 1 positive definite, a highly compliant torsional spring (k_b) can be attached to the output gear. This will introduce a new natural frequency to the torsional system, which can be made sufficiently low so as not to affect the primary response. The influence of the additional spring is shown in Fig. 6. First, the dynamic response is found for the semi-definite system. Since $\delta(t)$ represents only the relative displacement between the pinion and gear, a steady response is obtained (Figs. 6*a*–*b*). Next, the response is computed for the system after addition of a soft spring ($k/k_b \approx 5\times10^5$) on the output gear side. A low frequency component can be seen (Figs. 6(*c*)–(*d*), but for the frequency range of interest, the two systems yield similar results. Subsequently, the error can be reduced to a desired value by increasing the stiffness ratio.

Another important characteristic of sliding friction is that such forces are nonconservative in nature. Most existing analytical models retain the underlying assumption of a time-invariant input and output torques proportional to the gear ratio. Clearly, this is not consistent with the principle of energy conservation [7], as shown below. The energy loss ΔE_L during a mesh cycle is given by $\Delta E_L=\int_0^{t_c}(\tilde{T}_p\tilde{\theta}_p-\tilde{T}_g\tilde{\theta}_g)dt$. If T_p and T_g are taken as constant parameters, then the equation reduces to $\Delta E_L=T_p\int\tilde{\theta}_p dt - T_g\int\tilde{\theta}_g dt\equiv 0$. Hence it is not possible to account for the energy losses caused by sliding friction. The configuration described in the previous section, wherein the output gear was attached with a soft spring, can overcome this problem as well. In such a case, the input torque is assumed to be known whereas the external torque on output gear is reactive, operating through the torsional spring. Alternatively, the output torque may be held constant and excitation may be applied on the pinion. Thus by introducing an additional degree of freedom and fixing the output gear to a fixed rigid base via a compliant member, both the problems of semi-definiteness and energy balance can be resolved. In Fig. 7, the same two cases are analyzed as Fig. 6 and the input power to the system is plotted on the ordinate. When the external torques are assumed constant (Fig. 7(*a*)), the power term shows a periodicity

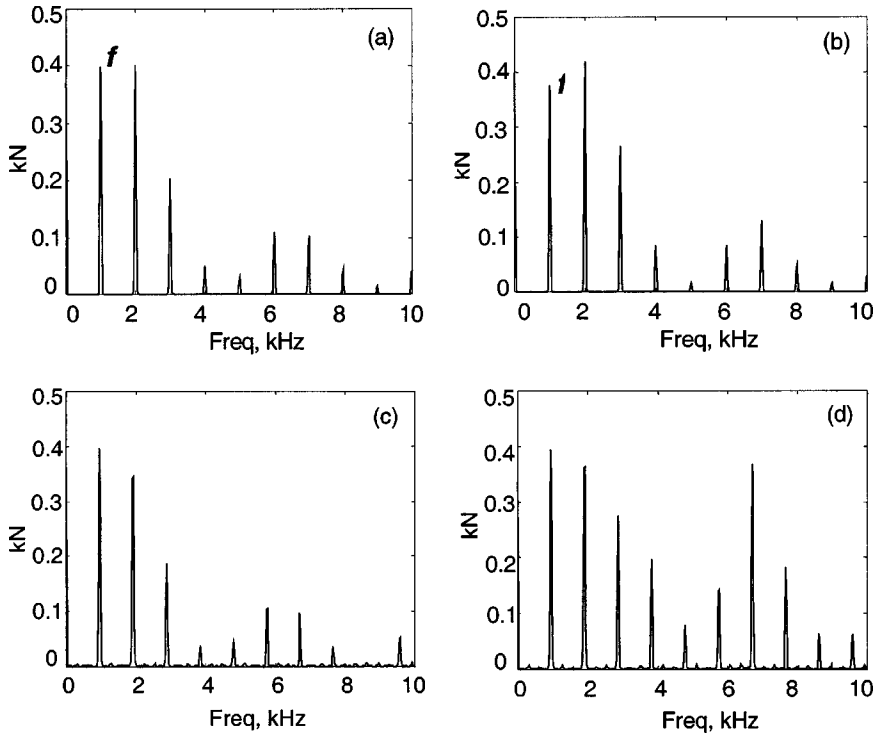

Fig. 5 Spectra of total friction force on when static and dynamic mesh forces are considered at $\Gamma=1.532$, $\mu=0.1$ and $\zeta=0.01$. (*a*) F_f calculated using N, at $\Omega_p=2400$ rpm (nonresonant condition); (*b*) F_f using F_{mesh}, at $\Omega_p=2400$ rpm; (*c*) F_f using N, at $\Omega_p=2300$ rpm (resonant condition); (*d*) F_f using F_{mesh}, at $\Omega_p=2300$ rpm.

with meshing frequency, but the mean value of power is zero. Conversely, when the output gear is fixed with a soft spring, the mean value of input power is 629 Watts, which compensates for the resistive loss due to the sliding friction.

$$J_e\ddot{\delta}+c_e\dot{\delta}+k_e\delta=T_e+\left(k_e+c_e\frac{d}{dt}\right)\sum_{i=1}^{n}\delta_{st,i}\cos(i\omega_{\text{mesh}}t+\phi_{\delta,i})+\sum_{i=1}^{n}T_{f,eq,i}\cos(i\omega_{\text{mesh}}t+\phi_{f,i}) \tag{10}$$

Linear Time-Invariant (LTI) System

In a gear mesh cycle, there is a significant variation in stiffness and damping. However, Ozguven and Houser [13] used a series expansion of meshing compliance and treated the gears as an equivalent linear time-invariant (LTI) system, where the stiffness variations are incorporated as higher harmonics of transmission error excitation. With this method, a good approximation is achieved for predicting the dynamic response over a wide frequency range. The time-averaged mean stiffness k_{mean} is calculated as $k_{\text{mean}}=\langle k(t)\rangle_t=k_{\max}(\Gamma-1)+k_{\min}(-\Gamma+2)$. The simplest approach to incorporate friction in this LTI system uses energy balance, wherein the frictional loss is simulated by introducing an energy equivalent viscous damping at the gear mesh [12]. For one meshing cycle, the energy loss is given by $\int\Sigma_{i=1}^{[\Gamma]}\mu_i N_i\xi_i d\theta_i=\int\tilde{T}_p\cdot d\tilde{\theta}_p$. Clearly, this method has limited applications, since only torsional dynamics are affected by the damping term. In reality, there will be significant dynamic forces in the η-direction. To account for these, F_f is represented by its Fourier expansion, so that it affects both the torsional dynamics and translation in the sliding direction. Thus the equation of motion in the torsional direction can be written as follows, where subscript e denotes an equivalent parameter in consistent units, and all other symbols have their usual meaning. The second and third terms in Eq. (10) represent the static loaded transmission error and friction respectively.

Linear Time-Varying (LTV) System Model

Although LTI analysis may give satisfactory results under many conditions, it has certain limitations, such as its inability to detect dynamic interactions amongst system parameters like friction and meshing stiffness variations. Furthermore, if parametric resonances, sub-harmonic response etc. is of interest, then the periodic properties of the system must be considered. Many studies in the past [3,5] have considered the friction between gear teeth as a time-varying function, such that the sliding velocity is determined solely from the kinematic considerations. A problem thus defined takes the form of a linear time-varying (LTV) system. For the dynamic system of Fig. 1, the equations of torsional motion can be written for the pinion and the gear as follows, where $T_{f,p}$ and $T_{f,g}$ can be derived using Eq. (9).

$$J_p\ddot{\theta}_p+c(\dot{\delta}-\dot{\varepsilon})R_p+k(\delta-\varepsilon)R_p=T_p+T_{f,p} \tag{11}$$

$$J_g\ddot{\theta}_g+c(\dot{\delta}+\dot{\varepsilon})R_g+k(\delta+\varepsilon)R_g=-T_g+T_{f,g} \tag{12}$$

By using the definition of δ, Eqs. (11–12) reduce to a single equation. For the LTV problem, the parametric variations are considered to be explicit functions of the time t, instead of the spatial value α. With this assumption, these parameters can be expressed as follows.

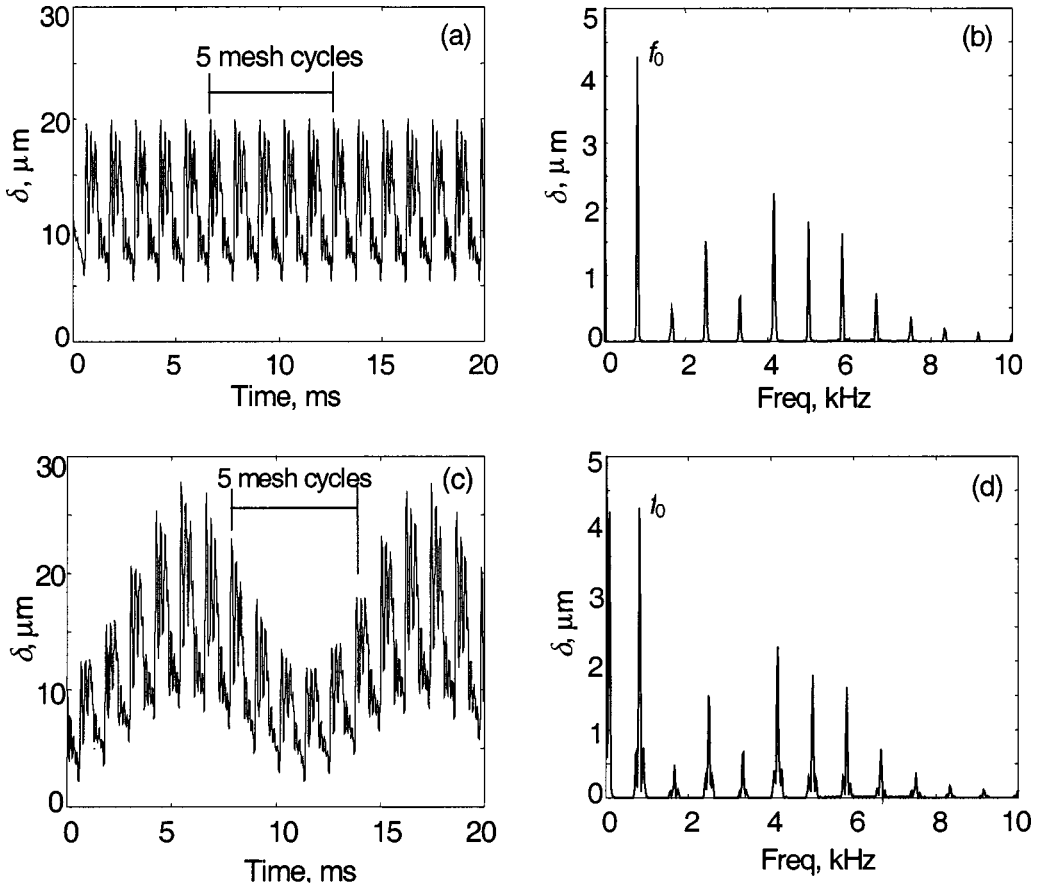

Fig. 6 Dynamic response $\delta(t)$ for 2000 rpm, ζ=.05, Γ=1.473, μ=0.1, $k/k_b=5\times10^5$ (*a*) Semi-positive definite system: time response; (*b*) Semi-positive definite system: frequency spectrum; (*c*) Positive definite system with extra spring: time response; (*d*) Positive definite system with extra spring: frequency spectrum.

(a) Load distribution $N_i(t)$:

$$N_1(t)=N_2(t)=N/2; \quad 0\leqslant t<t_a$$
$$N_1(t)=0; \quad N_2(t)=N; \quad t_a\leqslant t<t_c \tag{13a,b}$$

Here, total normal load $N=T_p/R_p$

(b) Mesh stiffness $k(t)$

$$k(t)=k_{\max}; \quad 0\leqslant t<t_a$$
$$k(t)=k_{\min}; \quad t_a\leqslant t<t_c \tag{14a,b}$$

(c) Coefficient of friction $\mu_i(t)$

$$\mu_1=+\mu_0\,\mathrm{sgn}(t-t_a); \quad 0\leqslant t<t_a$$
$$\mu_2=-\mu_0\,\mathrm{sgn}(t-t_b); \quad \forall t \tag{15a,b}$$

T_f will be given by $T_{f,i,j}=\gamma_{i,j}+\beta_{i,j}t$, where parameters γ and β depend upon the tribological conditions and meshing kinematics and subscripts i and j represent the tooth number and time interval respectively. The expression for sliding velocity simplifies to $V_{s,i}=\alpha_{p,i}R_p\Omega_p-\alpha_{g,i}R_g\Omega_g$.

Nonlinear Characteristics

So far, the sliding non-linearities in the system have been ignored. In a real system, friction mechanism exhibits an implicit non-linearity, where the resistive force is a function of V_S, which in turn is a system output variable. Then μ and T_f can be determined by:

$$\mu_i(t,\dot\theta_p,\dot\theta_g)=\mathrm{sgn}\left[\frac{\xi_{g,i}(t)(\Omega_g+\dot\theta_g)-\xi_{p,i}(t)(\Omega_p+\dot\theta_p)}{V_R}\right] \tag{16}$$

$$T_{f,i}(t,\dot\theta_p,\dot\theta_g)=\mu_i\xi_{p,i}(t)N_i(t) \tag{17}$$

In order to completely define this system, at least two independent variables must be chosen from θ_p, θ_g and δ. However, the system is still semi-definite and a stable solution for θ_p or θ_g may not be obtained. To resolve this conflict, two alternative methods are suggested. In the first approach, one of the gears is fixed via a spring to the base, as discussed earlier. In the second method, which may only be applied in numerical simulations, the equations are solved for the two angular displacement parameters θ_p and θ_g. Then a high-pass high order digital filter may be applied to both the parameters, so that the velocity corresponding to the rigid body motion is disregarded. This dynamic component of angular velocity is then used in Eq. (16).

Under normal conditions, V_S at the teeth has large cyclic variation, and the small vibratory component may not have a significant effect. However, near resonant conditions, large oscillations in angular velocity can cause multiple occurrences of sliding direction reversal within a mesh cycle. In Fig. 8(*a*), V_s is calculated using only the quasistatic angular velocities of the two gears. The variation shows straight lines due to linearly varying distances ξ_p and ξ_g. In Fig. 8*b*, the LTV model is used and the gear teeth pass the pitch point several times within a mesh cycle, especially for the 2nd tooth (upper curve). When the non-linear model is applied

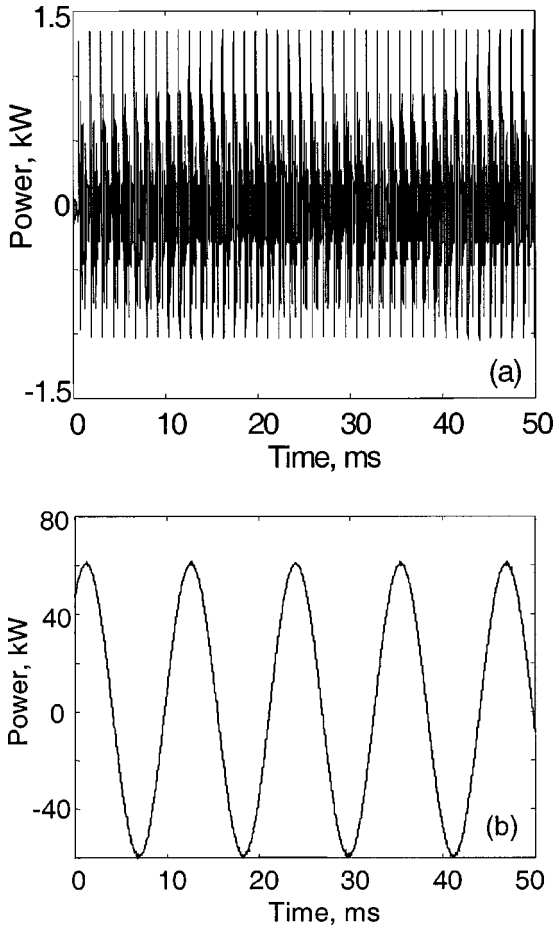

Fig. 7 Input power to the geared system. (*a*) With constant output and input torques, mean power=0; (*b*) With constant input torque and spring attached to output gear, mean power =629 Watts (equivalent to energy loss due to friction).

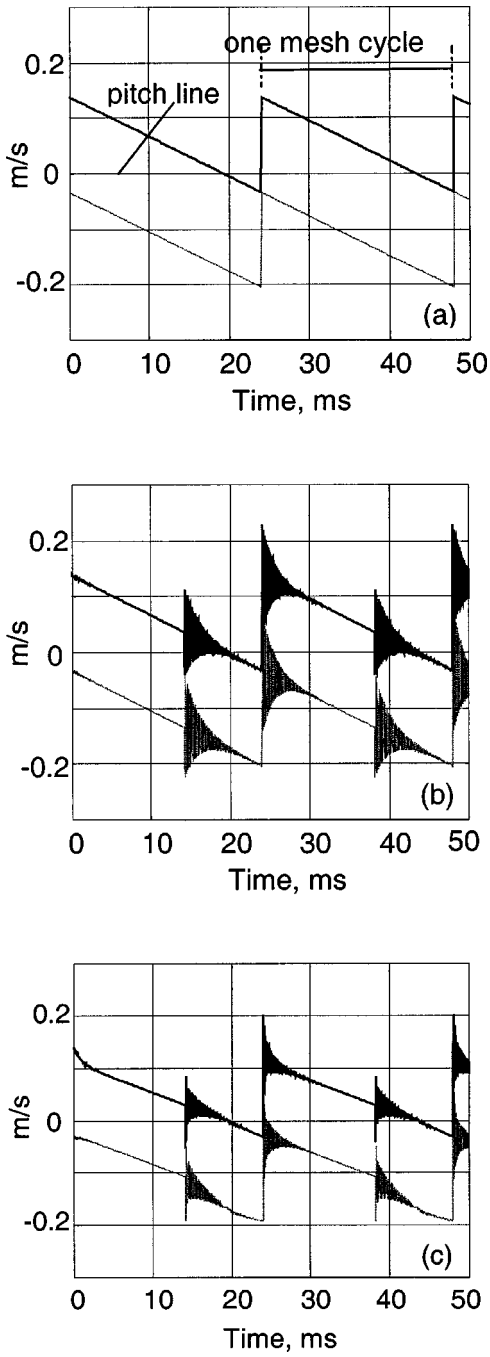

Fig. 8 Variation of sliding speed for the three friction models. (*a*) V_S for quasistatic case; (*b*) V_s for LTV model; (*c*) V_s with nonlinear friction. Key: —— 1st tooth, — — — 2nd tooth.

(Fig. 8(*c*)), the multiple pitch-point crossings impart significant energy dissipation and hence the magnitude of vibrations is considerably reduced.

The corresponding values of μ on the two teeth are shown in Fig. 9. With the LTV model, μ shows the same periodicity as the meshing frequency. However with the NLTV model, both the gear teeth show extra variations in the plot of μ, which become evident as higher harmonic components in the dynamic system. Apart from resonant conditions, two other parameters dictate how nonlinear μ will influence the response. The first is the phasing between the transition point (lowest point of single tooth contact) and the pitch point, i.e. t_a and t_b. This is due to the impulse-like excitation at time instant t_a, associated with the sudden change in meshing stiffness. Clearly, the farther t_b is from t_a, the less is the likelihood of the impulse response causing zero-velocity crossing. The second factor is the mean rotational speeds of the mating gears. Again, if this speed is maintained sufficiently high, the point t_a moves away from the pitch point and the nonlinearities may not have any significant dynamic effect.

Solution Methodology

Based on the complexity of the system and specific research objectives, alternative solution methodologies are applied. Broadly, these can be categorized as analytical, semi-analytical and numerical techniques. As the system equations become more intricate, such as in the case of multiple non-linearities, fully analytical solutions become intractable and they have to yield to numerical integrations. In this section, these methods are compared in the context of previously described torsional gear dynamic model incorporating sliding friction. For the simple case of an LTI system, there exist various time and frequency domain methods, including modal synthesis, harmonic solutions and Laplacian formulations. Here friction torque must be expressed as an external excitation and k shall be linearized about its time-averaged value. Since fully analytical solutions can easily be obtained even for fairly large LTI systems, such methods are not discussed here exclusively.

In order to find the time domain solution for an LTV system, Floquet theory [8,18] provides a fully analytical method. First, all the system parameters and excitations are defined in three piecewise continuous regimes within a tooth mesh cycle and the corre-

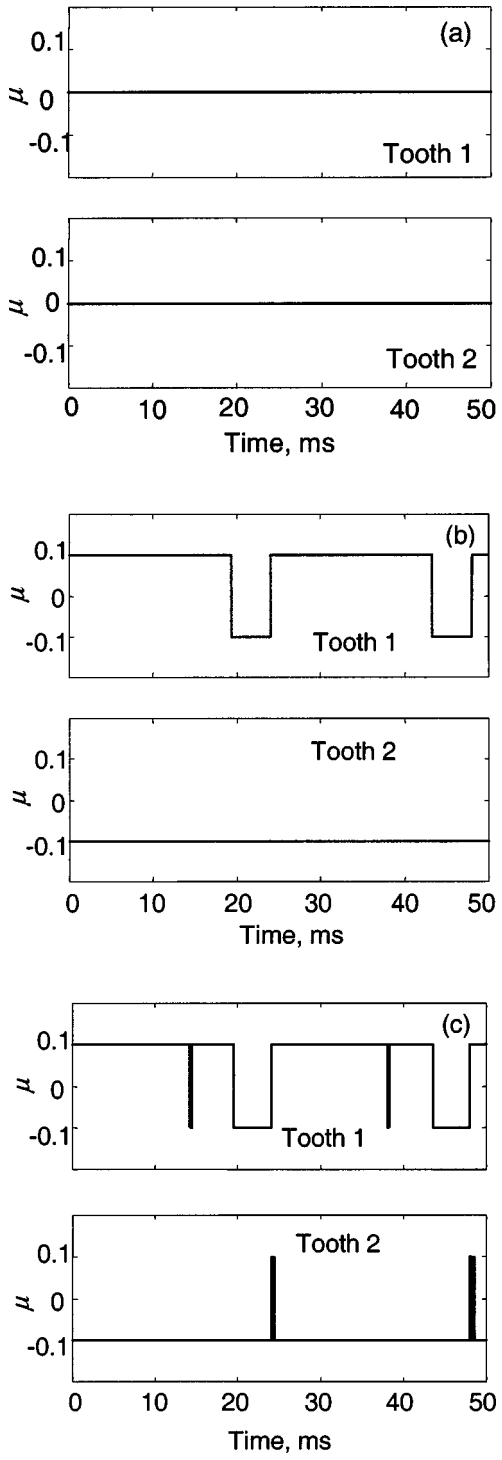

Fig. 9 Variation in coefficient of friction for different models at Ω_p=100 rpm, μ=0.1, Γ=1.590, ζ=0.01. (*a*) No friction; (*b*) Assumed variation corresponding to Fig. 7(*b*); (*c*) Actual variation corresponding to Fig. 7c.

sponding equations of motion are written. Two kinds of variations in sliding forces are considered, as discussed previously, such that formulation A is based on the quasistatic time-averaged transmitted torque, which leads to $F_f=\mu_i N$. Formulation B is based on the dynamic mesh forces, and is given by $F_f=\mu_i(k(\delta-\varepsilon)+c(\dot{\delta}-\dot{\varepsilon}))$. For formulation A, the system can be represented as the damped Meissner equation. Each segment of the piecewise linear system may be expressed in a general form as follows, where m_e, c_e and k_e are equivalent dynamic parameters. The homogenous part of Eq. (18) is independent of friction, thus effectively reducing the problem into a general second order equation for each time interval.

$$m_e\ddot{\delta}+c_e\dot{\delta}+k_e\delta(t)=\sum F_e(t) \tag{18}$$

For formulation B, the left hand side of the equation contains products of μ and $\xi_{p,i}(t)$, which is given by $\xi_{p,i}(t)=(\Omega_p t+\alpha_i+\alpha_0)R_p$. Consequently, the general form of the equations of motion consists of triangular coefficients, as shown below:

$$m_e\ddot{\delta}+c_e(1+\beta_c t)\dot{\delta}+k_e(1+\beta_k t)\delta(t)=\sum F_e(t) \tag{19}$$

In addition to friction, there are two other excitations, namely the mean load that acts via the parametric excitation and a displacement function ε due to profile variations. These can be generically represented by the mean torque $F(t)\approx T_0$, profile error $F(t)\approx k_e R_e \Sigma_i \varepsilon_i \cos(i\Omega\tau+\phi_i)$, and friction torque: $F_j(t)\approx\beta_{1,j}+\beta_{2,j}\tau$. Here j stands for each continuous interval, and R_e and k_e are the equivalent base radius and stiffness parameters respectively.

For formulation A, the Wronskian matrix **W** for each subinterval consists entirely of exponential functions. When formulation B is applied, both stiffness and damping coefficients take the sawtooth form and no analytical solutions exist for this problem. However, by ignoring the damping term and with appropriate substitution of variables, the equations converge to the form of Stokes equation [18]. One possible solution to this problem is given by a pair of Bessel functions of order 1/3 and $-1/3$. Thus, by accumulating the Wronskian for all individual time intervals, the state transition matrix for one complete mesh period is calculated. With the system matrix and Wronskian known for the two formulations, the forced response of the system can be found using the Cauchy formulation, where vector **f** contains an arbitrary forcing function and **x** is the generalized displacement. Thus, the solution is found in two distinct parts, namely for integral number of mesh cycles and that for the last cycle, as already reported by us [8].

$$\mathbf{x}(t)=\mathbf{W}(t)\mathbf{W}^{-1}(0)x(0)+\int_0^t \mathbf{W}(t)\mathbf{W}^{-1}(\tau)\mathbf{f}(\tau)d\tau \tag{20}$$

Semi-Analytical Methods

Analytical methods like Floquet theory require an a-priori knowledge of closed-form solutions over the piecewise function definitions. Furthermore, the formulation becomes very tedious, sometimes intractable, as more realistic and intricate function for $\mu(t)$ and $k(t)$ or system nonlinearities are considered. Some of these limitations are overcome with the application of semi-analytical methods. A number of studies have been carried out by researchers such as Padmanabhan and Singh [11], wherein Galerkin techniques have been applied to solve a variety of gear dynamic problems, such as those including parametric variations and clearance nonlinearities. For systems incorporating sliding friction, similar approach can be followed [15] to find the frequency-domain solutions. For instance, the dynamic response can be assumed to consist of n harmonics $(\omega,2\omega\ldots n\omega)$ of the tooth meshing frequency ω and m super-harmonics of the first subharmonic term, i.e. 0.5ω, $1.5\omega\ldots(m-0.5)\omega$. Thus, the total transmission error $\delta(t)$ can be expressed as $\delta(t)=\delta_h(t)+\delta_u(t)$, where the harmonic (δ_h) and sub-harmonic (δ_u) terms are given as follows:

$$\delta_h(t)=a_{\delta 0}+\sum_{i=1}^{n_h} a_{\delta i}\cos(i\omega t)+\sum_{i=1}^{n_h} b_{\delta i}\sin(i\omega t) \tag{21}$$

$$\delta_u(t)=\sum_{i=1}^{n_u} c_{\delta i}\cos((i-0.5)\omega t)+\sum_{i=1}^{n_u} d_{\delta i}\sin((i-0.5)\omega t) \tag{22}$$

Each of the time varying parameters like k, c, ε and F_f is expanded by Fourier series. All of these terms have the same periodicity of one tooth meshing cycle. After balancing the similar harmonic terms, the following equation is obtained:

$$[K_h(\omega)][a_{\delta 0}\ \ a_{\delta 1}\ldots a_{\delta n}\ \ b_{\delta 1}\ldots b_{\delta n}]^T=\{F(\omega)\} \tag{23}$$

Here, $K_h(\omega)$ is a square matrix of dimension $(2n+1)$, consisting of stiffness and damping terms. Similarly, $F(\omega)$ is the equivalent force vector comprising of profiles errors, external load and friction terms. Equation (23) can now be applied to solve for the coefficients of δ. The term $a_{\delta 0}$ appears as the mean deflection due to the external time-variant torque. The results obtained using the above mention harmonic balance method (HBM) compare well with the values obtained from numerical integration for the first harmonic, although the errors grow for higher harmonics.

Solution to a Nonlinear Problem

For analysis of non-linearities in gears, Blankenship and Singh [12] assumed that the stability can largely be determined by the response at the first harmonic of the excitation frequency. Such a hypothesis does not hold when a significant periodic variation is also present. Consequently, a higher order multi-term harmonic balance must be employed. Padmanabhan et al. [19] have investigated some computational issues associated with such systems and solution methods. Consider Eq. (17), where μ, F_{mesh} and ξ are further represented using Fourier expansions. Furthermore, the signum (sgn) function can be expressed in its Fourier form [20] as follows:

$$\text{sgn}(x)=\frac{4}{\pi}\left[\sum_{m=0}^{n_\mu}\frac{\sin(2m+1)x}{2m+1}\right] \tag{24}$$

This will lead to 5th order products in the multi-harmonic terms, whose numbers will further multiply when sub-harmonic response is also considered Additionally, the non-linear system comprises of two simultaneous equations and the number of terms will increase accordingly. For example, if n harmonic terms are considered in the solution, then the number of terms in the expanded equation is approximately $100(2n+1)^7$. Thus, even if a single harmonic is considered, there will be $O(10^5)$ terms in the expression. Such a complex expression is obviously intractable for the application of HBM. Note that a clearance-type system can be represented fairly well using a single-harmonic defining function. Furthermore, this function acts directly on the response variable δ of the system. Conversely, sliding friction is associated with a sudden change in value at the pitch point and multiple harmonic terms must be considered to obtain a realistic approximation. This situation is further complicated by the argument of the function, which includes the angular velocities of the pinion and gear, as well as the time-varying parameters ξ_p and ξ_g, as shown in Eq. (16). Thus the nature of the implicit non-linearity in a gear dynamic problem with friction results in far more intricate formulation, thus largely precluding a fully analytical treatment. Consequently, numerical integration is applied in the following sections for the NLTV system.

Comparative Analysis of LTI, LTV and NLTV Models

In this section, some results from the three formulations are presented. First, Fig. 10 shows the time-domain response due to friction as well as combined excitation. To isolate the friction effect in Fig. 10(b), $k(t)$ has been replaced by a time-averaged stiffness. This demonstrates that friction has a small but distinct contribution to the overall dynamic behavior.

To illustrate the difference between the three formulations, numerical simulation is carried out at very low rotational speed,

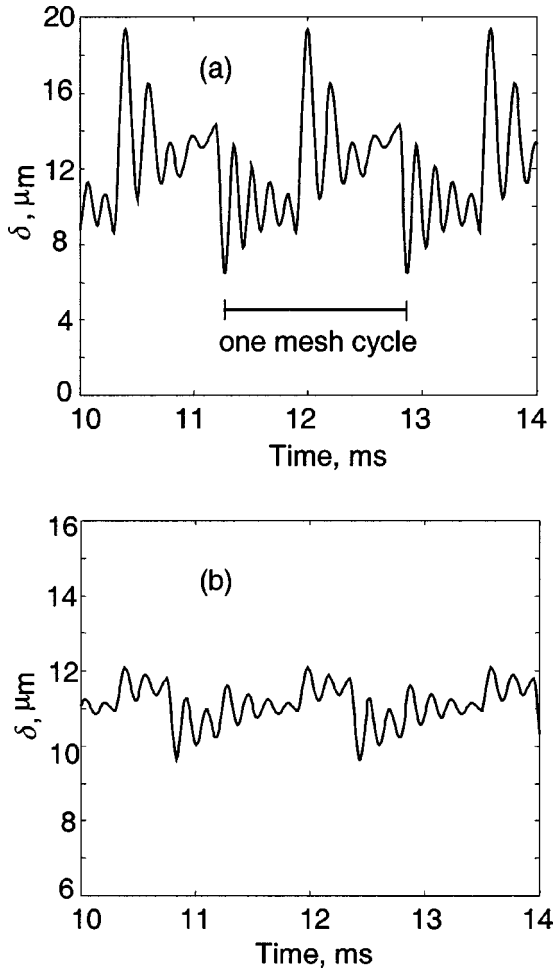

Fig. 10 Sample response for δ due to individual and combined excitations. (*a*) All excitations combined; (*b*) Only friction excitation $T_f(t)$.

because the non-linear effects are most pronounced under these conditions. Three different cases are analyzed and the results are shown in Fig. 11 in terms of δ. In Fig. 11(a) there is no sliding friction and the only excitation is caused by the sudden changes in mesh stiffness. On including friction as an LTV parameter, an additional impulsive effect is observed at the pitch point, as shown in Fig. 11(b). When the same system is analyzed with non-linearities (Fig. 11(c)), the rapid oscillations near the pitch point result in significant dampening of vibrations. However, the rest of the graph largely remains unaffected.

A strong influence of friction-induced non-linearity can be seen near resonant conditions. Figure 12(a) shows the divergent response for an LTV system lying in an unstable zone, corresponding to saddle-node bifurcation instability. When the same conditions are applied to an NLTV system, the time-domain response exhibits a long-term stability, as shown in Fig. 12(b). For these simulations, a low viscous damping coefficient of $\xi=0.001$ is used and the static deflection of the gear teeth with $\dot{\delta}=0$ is taken as the initial condition. When non-resonant operation conditions are applied (not shown here), the response of LTV and NLTV systems is nearly identical, implying that friction is acting primarily as an excitation and has no effect on the system stability. This indicates that under specific conditions, friction at teeth may have a stabilizing effect on the gear system.

The main cause for dynamic instabilities in gears is the parametric excitations due to variation in mesh stiffness and damping. Padmanabhan and Singh [11] have discussed three types of insta-

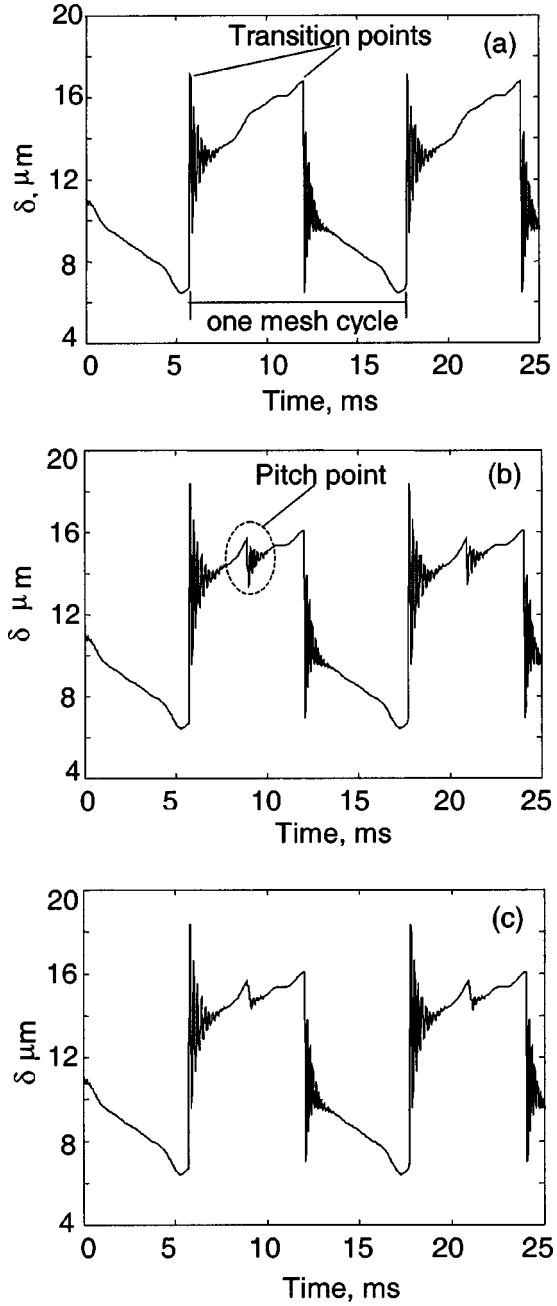

Fig. 11 Dynamic response for the three friction models in terms of δ, at $\Omega_p=200$ rpm, $\zeta=0.05$. (*a*) LTV system with $\mu_0=0$; (*b*) LTV system with $\mu_0=0.1$; (*c*) NLTV system with $\mu_0=0.1$.

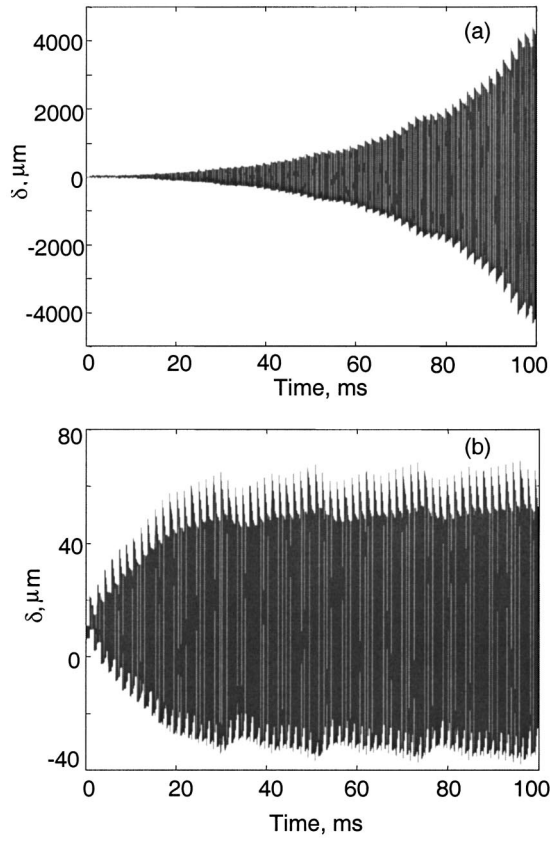

Fig. 12 Dynamic response $\delta(t)$ with LTV analysis, near resonance conditions for $\zeta=0.001$, $\mu=0.1$, $\Omega_p=1490$ rpm, $\Gamma=1.473$. (*a*) LTV system; (*b*) NLTV system.

bilities in gear applications, depending upon the eigenvalues of the system matrix. Richards [18] has shown that a sufficient condition for stability is that all the eigenvalues of the state transition matrix have an absolute value less than unity, or $|\lambda_i|<1\ \forall i$. Figure 13 shows the mapping of the maxima of $|\lambda_i|$ for the LTV system near one unstable zone, both for formulations A and B, as a function of rotational speed Ω_p and contact ratio Γ. Inclusion of friction only has the effect of shifting this region to the right, but the overall influence is negligible.

These results disagree with the hypothesis that sliding resistance has an equivalent damping property. In order to investigate this, the dynamic response of the nonlinear system is computed for several values of Γ and Ω_p, such that the system passes through multiple regimes of instability. The peak-to-peak transmission error is obtained for both the LTV and NLTV systems and their ratio $\gamma=\delta_{\mathrm{LTV}}/\delta_{\mathrm{NLTV}}$ is shown in the contour plots of Fig. 14. Here, a high value of the ratio indicates a smaller amplitude of response in the NLTV gear system. The zones at sub-harmonics like $\omega\approx 2\omega_n/3$ represent the period-doubling bifurcation whereas super-harmonics of ω correspond to saddle-node bifurcation instabilities. Since these results were obtained using numerical integration, no absolute criteria can be defined to identify the unstable zones. For the purpose of illustration, we have assumed a value of $\gamma>10^2$ as the threshold of instability. Accordingly, the inner two contours represent the zones where a stable response has been achieved due to friction non-linearity. The maximum influence of friction non-linearities is observed at the primary resonance, which occurs at $\Omega_p\approx 13{,}400$ rpm. Therefore, the difference between LTV and NLTV analyses appears to be significant onlynear unstable zones.

Conclusion

This article proposes alternative strategies for incorporating the phenomenon of sliding between gear teeth. First, a critical overview of existing methodologies and their underlying assumptions are presented. Even in a simplified torsional system, sliding friction has a significant influence on the dynamic response, especially at higher harmonics of the meshing frequency. The various underlying assumptions have a large impact on the dynamic response. Each approach has its own advantages and limitations, and their selection is dictated by the results of interest, such as time and frequency domain solutions, sub-harmonic and superharmonic response, short and long-term stability and so on. Our study shows a clear distinction between the excitation and damping effects of friction, and relates them to the time-varying and non-linear models. Friction non-linearities have the largest effect

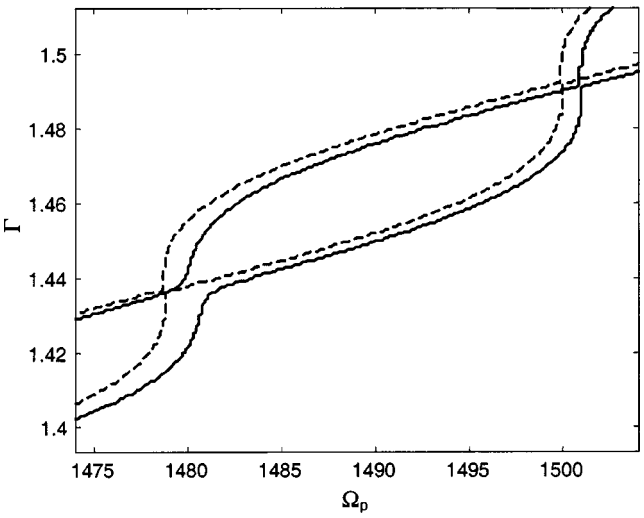

Fig. 13 Effect of Coulomb friction on instability zone, (——) with friction, (— — —) without friction (area enclosed within the curves is the unstable zone)

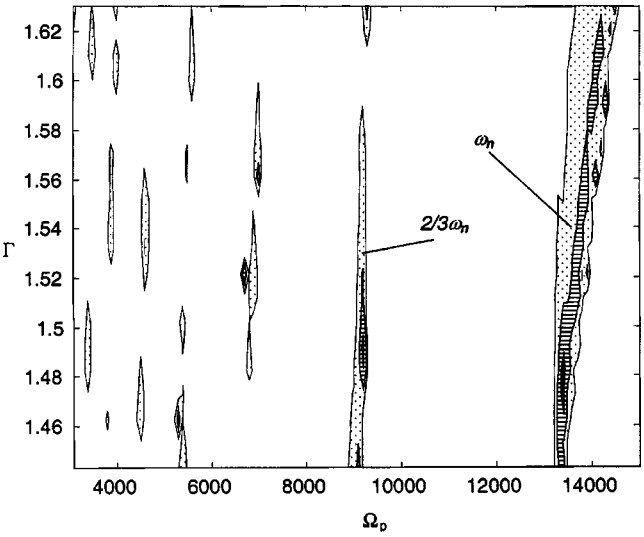

Fig. 14 Contours plots for the ratio γ of magnitude of δ between LTV and NLTV models, key: γ=3, γ=100, γ=100,000.

at very low speeds or near resonances, and hence can control the system stability. Various dynamic models are compared with respect to their applications, methodology, expected results and the assumptions with their consequences.

Given the importance of friction in the vibro-acoustic behavior of the geared systems, there is considerable potential for further research. The methods presented in this article may be extended to higher degree of freedom systems so that all aspects of friction mechanism may be investigated. Both meshing stiffness and the coefficient of friction need to have realistic representations. A meticulous contact analysis would provide a better load sharing amongst the teeth, as well as a distributed contact pressure over the tooth surface. To study the non-linear effects of sliding friction and its influence on different types of instabilities, a more rigorous analytical treatment is required. And finally, backlash nonlinearity and its interaction with the sliding characteristics at the tooth interface could be analyzed.

References

[1] Martin, K. F., 1978, ''A Review of Friction Predictions in Gear Teeth,'' Wear, **49**, pp. 201–238.

[2] Kelley, B. W., and Lemanski, A. J., 1967, ''Lubrication of Involute Gearing,'' Proc. Inst. Mech. Eng., **182**(3A), pp. 173–184.

[3] Radzimovsky, E., and Mirarefi, A., 1974, ''Dynamic Behavior of Gear Systems and Variation of Coefficient of Friction and Efficiency during the Engagement Cycle,'' ASME J. Eng. Ind., **74-DET-86**, pp. 1–7.

[4] Iida, H., Tamura, A., and Yamada, Y., 1985, ''Vibrational Characteristics of Friction between Gear Teeth,'' Bull. JSME, **28**(241), pp. 1512–1519.

[5] Borner, J., and Houser, D. R., 1996, ''Friction and Bending Moments as Gear Noise Excitations,'' Society of Automotive Engineers Technical Paper Series, 961816, pp. 1–8.

[6] Velex, P., and Cahouet, V., 2000, ''Experimental and Numerical Investigations on the Influence of Tooth Friction in Spur and Helical Gear Dynamics,'' *Proceedings of the 2000 ASME Design Engineering Technical Conferences*, DETC2000/PTG-14430, pp. 1–10.

[7] Vaishya, M., and Houser, D. R., 2000, ''Modeling and Analysis of Sliding Friction in Gear Dynamics,'' *Proceedings of the 2000 ASME Design Engineering Technical Conferences*, DETC2000/PTG-14431, pp. 1–10.

[8] Vaishya, M., and Singh, R., 2000, ''Analysis of Periodically Varying Gear Mesh Systems with Coulomb Friction using Floquet Theory,'' J. Sound Vib., **243**(3), pp. 525–545.

[9] Ozguven, H. N., and Houser, D. R., 1988, ''Mathematical Models used in Gear Dynamics—a Review,'' J. Sound Vib., **121**(3), pp. 383–411.

[10] Blankenship, G. W., and Singh, R., 1992, ''A Comparative Study of Selected Gear Mesh Force Interface Dynamic Models,'' *Proceedings of the 6th ASME International Power Transmission and Gearing Conference*, Vol. DE-43-1, pp. 137–146.

[11] Padmanabhan, C., and Singh, R., 1996, ''Analysis of Periodically Forced Nonlinear Hill's Oscillator with Application to a Geared System,'' J. Acoust. Soc. Am., **99**(1), pp. 324–334.

[12] Blankenship, G. W., and Singh, R., 1995, ''Analytical Solution for Modulation Sidebands Associated with a Class of Mechanical Oscillators,'' J. Sound Vib., **179**(1), pp. 13–36.

[13] Ozguven, H. N., and Houser, D. R., 1988, ''Dynamic Analysis of High Speed Gears by using Loaded Static Transmission Error,'' J. Sound Vib., **125**(1), pp. 71–83.

[14] Benton, M., and Seireg, A., 1978, ''Simulation of Resonances and Instability Conditions in Pinion-Gear Systems,'' ASME J. Mech. Des., **100**, pp. 26–32.

[15] Vaishya, M., and Singh, R., 2000, ''Sliding Friction Induced Non-linearity and Parametric Effects in Gear Dynamics,'' J. Sound Vib., **248**(4), pp. 671–694.

[16] Conry, T. F., and Seireg, A., 1973, ''A Mathematical Programming Technique for the Evaluation of Load Distribution and Optimal Modifications for Gear Systems,'' ASME J. Eng. Ind., pp. 1115–1122.

[17] Oh, S., Grosh, K., and Barber, J. R., 1998, ''Dynamic Behavior of Interacting Spur Gears: Energy Conservation,'' *Proceedings of the National Conference on Noise Control Engineering*, Institute of Noise Control Engineering, pp. 145–150.

[18] Richards, J. A., 1983, *Analysis of Periodically Time-Varying Systems*, Springer-Verlag, New York.

[19] Padmanabhan, C., Barlow, R. C., Rook, T. E., and Singh, R., 1995, ''Computational Issues Associated with Gear Rattle Analysis,'' ASME J. Mech. Des., **117**, pp. 185–192.

[20] Oberhettinger, F., 1973, *Fourier Expansions A Collection of Formulas*, Academic Press, Inc., New York.